Lecture Notes in Mechanical Engineering

Lecture Notes in Mechanical Engineering (LNME) publishes the latest developments in Mechanical Engineering—quickly, informally and with high quality. Original research reported in proceedings and post-proceedings represents the core of LNME. Volumes published in LNME embrace all aspects, subfields and new challenges of mechanical engineering. Topics in the series include:

- Engineering Design
- Machinery and Machine Elements
- Mechanical Structures and Stress Analysis
- Automotive Engineering
- Engine Technology
- Aerospace Technology and Astronautics
- Nanotechnology and Microengineering
- Control, Robotics, Mechatronics
- MEMS
- Theoretical and Applied Mechanics
- Dynamical Systems, Control
- Fluid Mechanics
- Engineering Thermodynamics, Heat and Mass Transfer
- Manufacturing
- Precision Engineering, Instrumentation, Measurement
- Materials Engineering
- Tribology and Surface Technology

To submit a proposal or request further information, please contact the Springer Editor of your location:

China: Ms. Ella Zhang at ella.zhang@springer.com
India: Priya Vyas at priya.vyas@springer.com
Rest of Asia, Australia, New Zealand: Swati Meherishi at swati.meherishi@springer.com
All other countries: Dr. Leontina Di Cecco at Leontina.dicecco@springer.com

To submit a proposal for a monograph, please check our Springer Tracts in Mechanical Engineering at https://link.springer.com/bookseries/11693 or contact Leontina.dicecco@springer.com

Indexed by SCOPUS. All books published in the series are submitted for consideration in Web of Science.

More information about this series at https://link.springer.com/bookseries/11236

Harshit K. Dave · Uday Shanker Dixit ·
Dumitru Nedelcu
Editors

Recent Advances in Manufacturing Processes and Systems

Select Proceedings of RAM 2021

Springer

Editors
Harshit K. Dave
Department of Mechanical Engineering
S. V. National Institute of Technology
Surat, Gujarat, India

Uday Shanker Dixit
Department of Mechanical Engineering
Indian Institute of Technology Guwahati
Guwahati, Assam, India

Dumitru Nedelcu
Gheorghe Asachi Technical
University of Iasi
Iasi, Romania

ISSN 2195-4356 ISSN 2195-4364 (electronic)
Lecture Notes in Mechanical Engineering
ISBN 978-981-16-7786-1 ISBN 978-981-16-7787-8 (eBook)
https://doi.org/10.1007/978-981-16-7787-8

Preface

Since 2010, Department of Mechanical Engineering at Sardar Vallabhbhai National Institute of Technology, Surat, has been organizing series of conferences on "Recent Advances in Manufacturing." In order to enable the sharing of knowledge in the areas of manufacturing technologies, we have organized six national conferences on "Recent Advances in Manufacturing" since 2010, and the first international conference on Recent Advances in Manufacturing (RAM-2020) was organized in July 2020. The conference is organized to bring the academicians, researchers and practicing engineers for sharing their experiences in the field of advance manufacturing. RAM-2021 aims to provide the opportunity for networking among participant institutes/organizations/industries to systematically confront the challenges in mutual areas of interest to advance manufacturing technology in these areas.

The proceedings volumes are published in the Springer series *Lecture Notes in Mechanical Engineering* in two volumes, viz. Volume 1—*Recent Advances in Manufacturing: Processes and Systems* and Volume 2—*Recent Advances in Manufacturing: Modeling and Optimization.* We also acknowledge the academic support from Prof. Dumitru Nedelcu, Prof. U. S. Dixit, Prof. J. Ramkumar and Prof. Panagiotis Kyratsis while editing both the volumes. In this volume, a total of 80 papers have been included in the domain of conventional and unconventional material removal processes, material forming processes, welding and joining processes, casting processes, additive manufacturing processes and characterization of composite materials.

As the entire world is facing the threat from corona pandemic, the international as well as interstate travel is restricted. However, we have tried our best to carve out a comprehensive schedule, keynote speakers, oral presentations in both online and offline mode, all of which will facilitate stimulating insightful discussions within the research community. In spite of such a pandemic situation, 181 participants have presented their findings and exchanged ideas related to manufacturing domain.

We are thankful to the conference organizing committee members, the advisory committee members, the reviewers, session chairs and the volunteers, without whose generous contributions this conference would not have been successfully conducted.

.

Most of all, we thank the participants for enriching the international conference with their active participation.

Surat, India

Dr. Shailendra Kumar
Organizing Secretary

Dr. Harshit K. Dave
Organizing Secretary, RAM-2021

Contents

About the Editors

Dr. Harshit K. Dave is currently working as an Associate Professor at the Department of Mechanical Engineering, S. V. National Institute of Technology, Surat. He obtained his B.E. (Mechanical) from Saurashtra University, Rajkot, and M.E. (Production) from M. S. University, Vadodara, and Ph.D. from SVNIT, Surat. His major areas of research interests include unconventional machining processes, micro-machining processes, machining of advanced materials, additive manufacturing processes, and modeling & optimization of machining processes, composite fabrication. He has published more than 50 papers in reputed international journals. Dr. Harshit Dave has carried out several research projects funded by DST, MHRD, and GUJCOST etc.

Dr. Uday Shanker Dixit is currently working as a Professor at Indian Institute of Technology, Guwahati. He earned his B.E. (Mechanical) from University of Roorkee in 1987 and M.Tech. (Mechanical) from IIT Kanpur, in 1993, and Ph.D. from IIT Kanpur in 1998. His current research interest is finite element method and soft computing applications in a wide variety of problems in manufacturing and design. He is also working in the domain of mechatronics. He holds 130 publications in reputed journals, 16 books and 38 book chapters. Dr. Uday Shanker has completed several sponsored projects and consultancy work sanctioned by various funding agencies.

Dr. Dumitru Nedelcu is currently working as a Professor at the Department of Machine Manufacturing Technology, Technical University of Iasi (TUIASI). He obtained his graduation in mechanical engineering from Polytechnic Institute of Iasi, Romania and Ph.D. from Technical University of Iasi, Romania. His major areas of research interests include fine mechanics technologies and technologies to obtain and process composite materials. Dr. Nedelcu Dumitru holds four patents and is the author of 60 refereed publications and 15 books. Over the years he got 17 national/international awards.

A Study on Residual Stress Distribution in Welded Joint of P91 and SS304H Steel Plate

Sachin Sirohi, P. K. Taraphdar, Prakash Kumar, and Chandan Pandey

Abstract The experimental study has been done to investigate the through thickness residual stress variation in P91/SS304H welds joint. The gas tungsten arc welding (GTAW) has been performed for joining of the dissimilar metal using the Ni-based ERNiCrMo-3 filler. The residual stress measurement was performed in the weld metal, SS304H HAZ and P92 HAZ. The results showed a considerable deviation in residual stresses along the thickness and in the transverse direction of the weldments. The PWHT showed a significant effect on magnitude and nature of the transverse and longitudinal residual stress for both weld metal and HAZ.

Keywords P91 · SS304H · IN625 · Residual stress · Welding

1 Introduction

The 9–12% Cr steel is used in boiler and turbine components to operate at higher temperature (600–650 °C) due to its attractive creep resistance at higher temperature [1, 2]. However, 9–12% Cr steels show the degradation in oxidation resistance at temperature more than 650 °C [1]. Hence, boiler components like reheater and superheater tubes with operating temperatures more than 650 °C are generally made

S. Sirohi (✉)
Department Mechanical Engineering, SRM IST NCR Campus, Modinagar 201204, India

P. K. Taraphdar
School of Mechanical Sciences, Indian Institute of Technology Bhubaneswar, Bhubaneswar 752050, India

P. Kumar
Department of Production Engineering, National Institute of Technology Tiruchirappalli, Tiruchirappalli 620015, India
e-mail: prakashkumar@nitt.edu

C. Pandey
Department of Mechanical Engineering, Indian Institute of Technology Jodhpur, Jodhpur 342037, India
e-mail: jscpandey@iitj.ac.in

H. K. Dave et al. (eds.), *Recent Advances in Manufacturing Processes and Systems*, Lecture Notes in Mechanical Engineering,
https://doi.org/10.1007/978-981-16-7787-8_1

of austenitic grade SS304L, SS304H steel, or Ni-based superalloy IN617, IN718 [3, 4]. Joining of these two steels requires to reduce the total operating cost of the power plant. The frequently used 9–12% Cr steel are P91, P911, and P92, which derived their strength by tempered martensite and carbide precipitates of type $M_{23}C_6$ and MX [5, 6]. In austenitic grade steel, the SS304L and SS304H are more commonly employed in power plants because of its high oxidation and corrosion resistance [7, 8]. Both P91 steel and SS304H steel shows the difference in thermo-physical and mechanical properties and chemical composition. The variation in coefficient of thermal expansion and thermal conductivity of these two steels creates the major problem during the joining and a high amount of residual stress is obtained along the welded joint [9, 10]. The high heat input and variation in composition and mechanical properties of these two steels results in poor structural integrity, as presented by the researchers [11–22]. The high amount of residual stresses and difference in mechanical properties along the welded joint leads to premature failure of the weld component. The diffusion of the elements along the weld metal and heat-affected zone (HAZ) interface was also observed during dissimilar welding of SS304H and P91 steel. The dissimilar joining is mainly concerned with the application of the heat input and filler metal. The welding of these two steel using the matching P91 filler has reported poor impact toughness due to the development of the fresh martensite in weld metal [10, 13]. For stainless steel grade filler, solidification cracking is reported as the major issue [23]. For joining the SS304H and P91 steel, Ni-based filler such as IN82, IN617, and IN625 has been reported as the best choice due to attractive creep properties at high-temperature [24, 25]. The other reasons behind the selection of the Ni-based filler are their thermal conductibility and thermal expansion coefficient, which lies in between SS304H and P91 steel and it also helps to stop the diffusion of the elements. Numerous research articles have been published on the use of Ni-based filler to join the P91 and SS304H steel. However, residual stress along the welded joint still exists, which can be minimized either by minimizing the heat input or performing the post-weld heat treatment (PWHT). However, a study related to the residual stress analysis of P91 and SS304H welded joint for Ni-based filler has not been found. The objective of this work is to examine the residual stress variation along the welded joint for the Ni-based IN625 filer. The effect of the PWHT on residual stress variation has also been studied and results obtained after PWHT, compared with the as-welded condition.

2 Work Material and Testing

The P91 and SS304H plate of thickness 8.5 mm were welded using the gas tungsten arc welding technique with the IN625 filler. After the welding, PWHT was employed at 760 °C for 2 h. The detail about the welding process parameters and groove design has been given into previously published work [26]. The design of groove, groove machined plate, and top and back side of the welded plate is revealed in Fig. 1a–c [26].

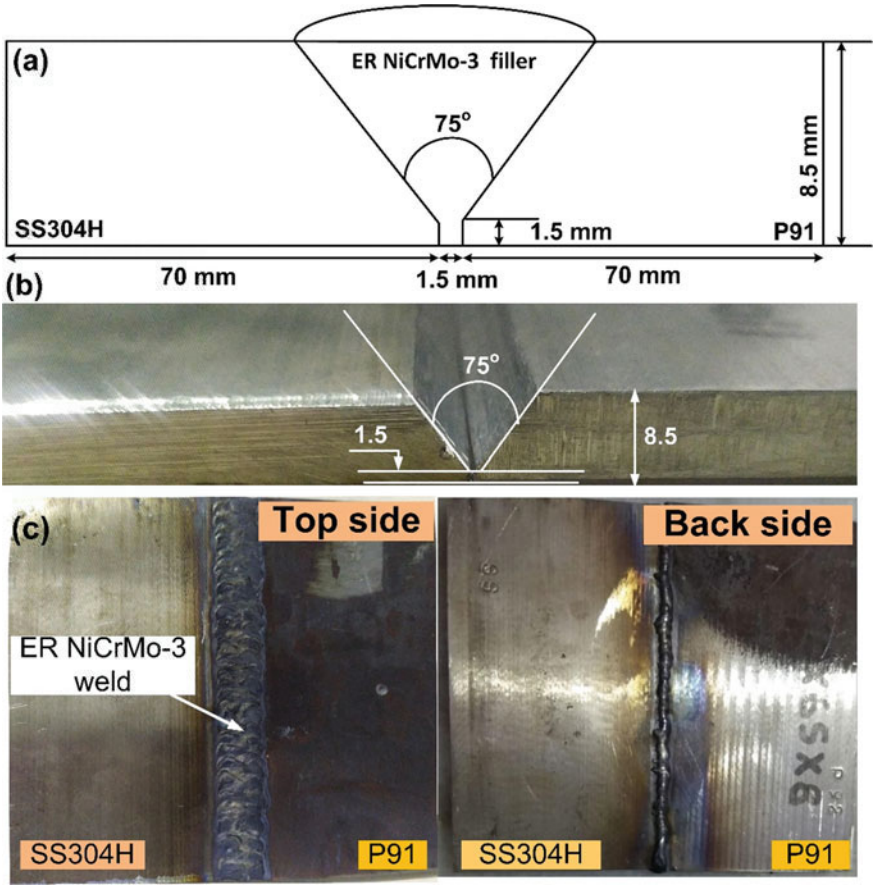

Fig. 1 **a** Groove details, **b** plate after machining the groove, **c** top and back side of the welded plate

After joining and PWHT, through-hole thickness measurement was performed. For the measurement of residual stress distribution in the weld zone and the HAZ, deep hole drilling (DHD) method was used. Four essential steps are followed in the DHD technique, which is revealed in Fig. 2. In first step, a through thickness hole of diameter 3 mm was drilled at desired position, i.e., weld metal or HAZ. In the second, the measurement of reference hole diameter ($d(\theta)$) was conducted with an air probe in 1 mm depth intervals across the thickness in the transverse and longitudinal directions. In third step, trepanning was done for reference hole by using the electro-discharge machining to relax the present locked-in stresses surrounding the reference hole. Subsequently, in the final step, remeasurement of the reference hole diameter $\left(d'(\theta)\right)$ was performed with the air probe at the previous locations through the thickness following similar directions as before. In-plane residual stress magnitude was estimated with the help of the variation in reference hole diameter $\left(\Delta d(\theta) = d'(\theta) - d(\theta)\right)$. The normalized strain $\varepsilon(\theta)$ is given below,

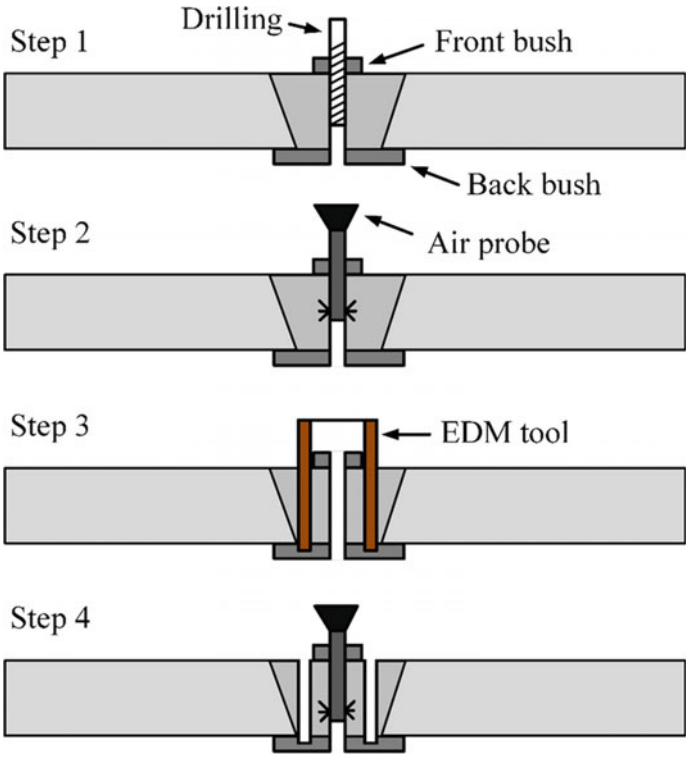

Fig. 2 Steps used in deep hole drilling method [30]

$$\varepsilon(\theta) = \frac{\Delta d(\theta)}{d(\theta)} = -\frac{1}{E}\left[\sigma_x p(\theta) + \sigma_y q(\theta) + \sigma_{xy} r(\theta) - \mu\sigma_z\right] \tag{1}$$

$$\varepsilon_z = -\frac{1}{E}\left[-\sigma_z - \mu\left(\sigma_y + \sigma_x\right)\right] \tag{2}$$

where $p(\theta) = 1 + 2\cos 2\theta$, $q(\theta) = 1 - 2\cos 2\theta$, $r(\theta) = 4\sin 2\theta$ and ε_z is the measured axial strain derived during the trepanning process. The plane stress condition is followed while determining residual stresses using the DHD technique, resulting in the conversion of the σ_z to zero. Measurements of reference hole were performed at n angles ($\theta = \theta_1, \ldots, \theta_i, \ldots, \theta_N$) around the hole. Thus, Eq. 1 can be rewritten as,

$$\varepsilon(\theta) = \frac{\Delta d(\theta)}{d(\theta)} = -\frac{1}{E}\left[\sigma_x p(\theta) + \sigma_y q(\theta) + \sigma_{xy} r(\theta)\right] \tag{3}$$

Here, the x-direction meets with the angular direction $\theta = 0°$. Equation 3 can be reframed in a matrix format as shown below,

$$\overline{\varepsilon} = -\frac{1}{E}\mathbf{M} \times \sigma \tag{4}$$

where

$$\overline{\varepsilon} = \begin{bmatrix} \overline{\varepsilon}(\theta_1) \\ \vdots \\ \overline{\varepsilon}(\theta_i) \\ \vdots \\ \overline{\varepsilon}(\theta_N) \end{bmatrix}, \ \mathbf{M} = \begin{bmatrix} p(\theta_1) & q(\theta_1) & r(\theta_1) \\ \vdots & \vdots & \vdots \\ p(\theta_i) & q(\theta_i) & r(\theta_i) \\ \vdots & \vdots & \vdots \\ p(\theta_N) & q(\theta_N) & r(\theta_N) \end{bmatrix} \text{ and } \sigma = \begin{bmatrix} \sigma_x \\ \sigma_y \\ \sigma_{xy} \end{bmatrix} \tag{5}$$

Finally, using Eq. 6, the residual stresses magnitude can be determined.

$$\hat{\sigma} = -E\mathbf{M}^* \times \overline{\mathbf{u}} \tag{6}$$

where

$$\mathbf{M^*} = \left(\mathbf{M^T} \times \boldsymbol{M}\right)^{-1} \times \mathbf{M^T} \tag{7}$$

Here, $\hat{\sigma}$ = favorable stress vector; $\mathbf{M^*}$ = pseudo inverse of matrix $\mathbf{M}$ [27].

Furthermore, Mahapatra and his co-workers made the above-mentioned calculation simpler [28, 29].

The longitudinal (ε_x) and transverse (ε_y) strain is calculated by simply placing $\theta = 0^0$ and $\theta = 90^0$, respectively, in Eq. 3, as shown in Eqs. 8 and 9.

$$\varepsilon_x = \frac{\Delta d_x}{d_x} = -\frac{1}{E}\left[3\sigma_x - \sigma_y\right] \tag{8}$$

$$\varepsilon_y = \frac{\Delta d_y}{d_y} = -\frac{1}{E}\left[3\sigma_y - \sigma_x\right] \tag{9}$$

For uniaxial stress,σ_y will be zero in Eq. 8,

$$\varepsilon_x = \frac{\Delta d_x}{d_x} = -\frac{1}{E}[3\sigma_x] \tag{10}$$

Equations 8 and 9 were used to quantify the in-plane bi-axial longitudinal and transverse residual stress fields.

3 Results and Discussion

The distribution of residual stress along the thickness for a different region of the weldments is shown in Fig. 3. In the weld metal, the maximum value of the longitudinal residual stress was obtained at a depth of 6 mm from the upper surface, and it was almost constant up to a depth of 5 mm. For weld metal, the maximum value of the longitudinal residual stress in as-welded condition approached 250 MPa, which was higher than the maximum value of the transverse residual stresses of 165 MPa (Fig. 3a). After conducting the PWHT, it was found that the tensile residual stress fields transformed into compressive stresses through the thickness. The induced compressive residual stress levels were found to be comparatively higher when IN625 was used as the filler material. The maximum compressive transverse and longitudinal residual stress magnitudes in the weld zone (IN625) after PWHT were found to be −123 and −295 MPa at a depth of 5 mm from the upper surface of the weld,

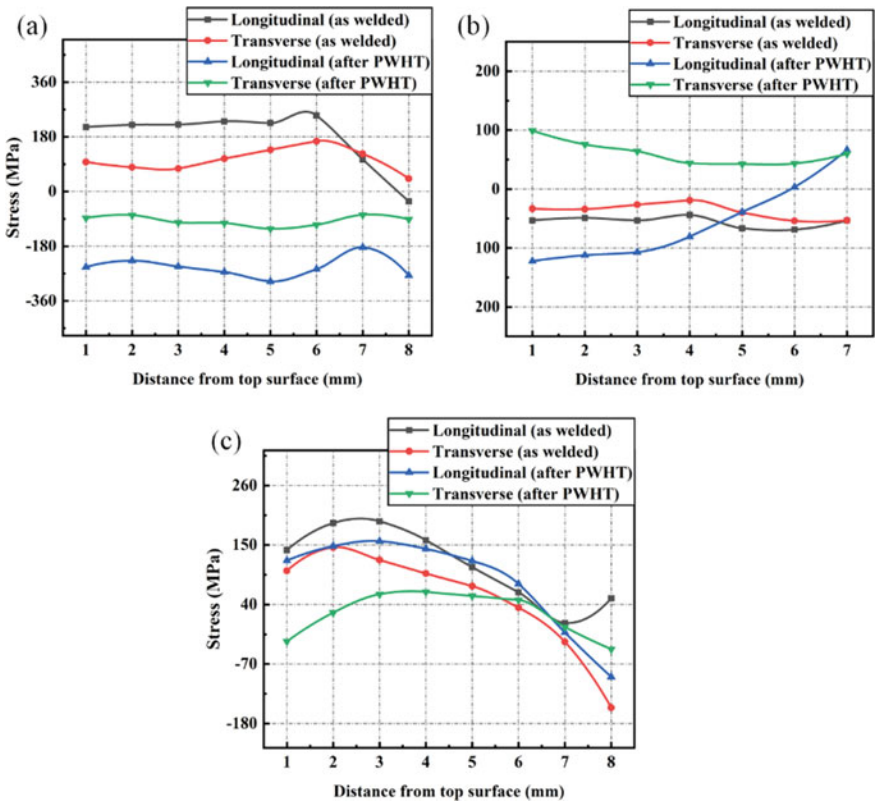

Fig. 3 Through thickness residual stress distribution in the weldment having IN625 as the filler material **a** weld zone, **b** P92 HAZ, **c** SS304H HAZ

respectively. Similar to the weld sample of IN617, the weldment of IN625 also exhibited compressive residual stresses in the HAZ of the P92 steel within a range of −19 to −70 MPa, Fig. 3b. However, following PWHT, the transverse residual stress trend moved into the tensile region, while the longitudinal residual stress trend dropped deeper into the compressive zone at the top surface, eventually becoming tensile at the bottom of the plate. The maximum longitudinal stress level of 193 MPa and maximum transverse residual stress level of 145 MPa were measured in the SS304H HAZ, as presented in Fig. 3c. The maximum value of transverse and longitudinal residual stresses in the SS304H HAZ decreased by 83 and 18%, respectively, after the PWHT, Fig. 3c.

In a comparison of the weld samples of IN617 and IN625, it was observed that the weld sample of IN625 exhibited a higher residual stress level in the weld zone, and consequently, after PWHT, it also produced a higher magnitude of compressive residual stresses in the weld zone. Both the weld samples had similar residual stress levels with marginal differences in the HAZ of P92 steel in the as-welded condition [31]. Noticeably, after PWHT, the transverse residual stress trend of the IN625 weld sample was found as tensile in nature, whereas in the IN617 weld sample, the transverse residual stress trend further moved deeper into the compressive zone after PWHT. In both cases, the longitudinal residual stress levels in the P92 HAZ increased in the compressive mode at the top surface. It was observed that the IN625 weld sample exhibited higher residual stress magnitudes in the HAZ of SS304H than the IN617 weld sample in both the longitudinal and transverse directions [31]. These residual stress levels in SS304H HAZ decreased by a certain amount after PWHT, with the transverse residual stress greatly reduced in both weld samples by an average of 80%. The differences in the thermal expansion coefficient and metallurgical properties of the corresponding dissimilar metals are directly responsible for the variations in the distribution of residual stress in these weld samples across the weld cross section.

4 Conclusion

1. The results showed a considerable deviation in residual stresses in transverse direction of the joint and along the thickness.
2. The maximum value of the longitudinal residual stress in weld metal was 250 MPa while the transverse residual stress was 165 MPa, for as-welded conditions and showed a substantial decrease in magnitude and nature after the PWHT.
3. For P91 HAZ, the compressive nature of the residual stresses was obtained throughout the depth in as-welded conditions. After the PWHT, longitudinal residual stress was measured in the root of the weld metal with a maximum magnitude of 67 MPa, which was tensile in nature. A tensile transverse residual stress was measured after the PWHT with a maximum value of 99 MPa at the top of the plate.

4. The maximum longitudinal and transverse residual stress levels in the SS304H HAZ were measured about 193 and 145 MPa, respectively, while a compressive nature of the transverse stress was measured in the root portion with a magnitude of 150 MPa. After the PWHT, a reduction was measured in residual stresses, and maximum longitudinal and transverse residual stress levels were 157 and 63 MPa, respectively.

References

Journal Article

1. Akram J, Kalvala PR, Misra M, Charit I (2017) Creep behavior of dissimilar metal weld joints between P91 and AISI 304. Mater Sci Eng A 688:396–406
2. Kumar S, Pandey C, Goyal A (2021) Microstructure and mechanical behavior of P91 steel dissimilar welded joints made with IN718 filler. Int J Press Vessels Pip 190: 104290
3. Dak G, Pandey C (2020) A critical review on dissimilar welds joint between martensitic and austenitic steel for power plant application. J Manuf Process 58:377–406
4. Abe F (2015) Research and development of heat-resistant materials for advanced USC power plants with steam temperatures of 700 °C and above. Engineering 1(2):211–224
5. Pandey C, Mahapatra MM, Kumar P, Saini N (2018) Some studies on P91 steel and their weldments. J Alloy Compd 743:332–364
6. Klueh RL (2005) Elevated temperature ferritic and martensitic steels and their application to future nuclear reactors. Int Mater Rev 50:287–310
7. Pandey C (2020) Mechanical and metallurgical characterization of dissimilar P92/SS304 L welded joints under varying heat treatment regimes. Metall Mater Trans A 51:2126–2142
8. Khodakov VD, Khodakov DV (2016) Structure and mechanism of formation of dissimilar welded joints in nuclear power plant made of austenitic and pearlitic steels. Weld Int 30(12):935–940
9. Williams JA (1984) Residual stresses in austenitic/ferritic transition joints fabricated with austenitic weld metal. High Temp Technol 2(3):135–140
10. Thakare JG, Pandey C, Mahapatra MM, Mulik RS (2019) An assessment for mechanical and microstructure behavior of dissimilar material welded joint between nuclear grade martensitic P91 and austenitic SS304 L steel. J Manuf Process 48:249–259
11. Pandey C, Mahapatra MM, Kumar P, Saini N (2018) Homogenization of P91 weldments using varying normalizing and tempering treatment. Mater Sci Eng, A 710:86–101
12. Shuo W, Limin W, Yi C, Shuping T (2018) Post-weld heat treatment and groove angles affect the mechanical properties of T92/Super 304H dissimilar steel weld joints. High Temp Mater Processes (Lond) 37(7):649–654
13. Falat L, Kepic J, Ciripova L, Sevc P, Dlouhy I (2016) The effects of postweld heat treatment and isothermal aging on T92 steel heat-affected zone mechanical properties of T92/TP316H dissimilar weldments. J Mater Res 31:1532–1543
14. Chen G, Song Y, Wang J, Liu J, Yu X, Hua J, Bai X, Zhang T, Zhang J, Tang W (2012) High-temperature short-term tensile test and creep rupture strength prediction of the T92/TP347H dissimilar steel weld joints. Eng Fail Anal 26:220–229
15. Pandey C, Mahapatra MM, Kumar P, Saini N (2018) Comparative study of autogenous tungsten inert gas welding and tungsten arc welding with filler wire for dissimilar P91 and P92 steel weld joint. Mater Sci Eng A 712:720–737

16. Deng J, Liang Z, Hui S, Zhao Q (2015) Aging treatment on the microstructures and mechanical properties of new groove T92/super 304H dissimilar steel joints. High Temp Mater Processes (Lond) 34(5):425–433
17. Vidyarthy RS, Kulkarni A, Dwivedi DK (2017) study of microstructure and mechanical property relationships of A-TIG welded P91–316L dissimilar steel joint. Mater Sci Eng A 695:249–257
18. Karthick K, Malarvizhi S, Balasubramanian V, Rao G (2018) Tensile properties variation across the dissimilar metal weld joint between modified 9Cr–1Mo ferritic steel and 316LN stainless steel at RT and 550 °C. Metallogr Microstruct Anal 7:209–221
19. Jula M, Dehmolaei R, Alavi Zaree SR (2018) The comparative evaluation of AISI 316/A387-Gr.91 steels dissimilar weld metal produced by CCGTAW and PCGTAW processes. J Manuf Process 36:272–280
20. Pańcikiewicz K, Świerczyńska A, Hućko P, Tumidajewicz M (2020) Laser dissimilar welding of AISI 430F and AISI 304 stainless steels. Materials 13(20):4540
21. Sirohi S., Pandey C, Goyal A (2020) Role of heat-treatment and filler on structure-property relationship of dissimilar welded joint of P22 and F69 steel. Fusion Eng Des 159: 111935
22. Sun Z, Moisio T (1993) Laser beam welding of austenitic/ferritic dissimilar steel joints using nickel based filler wire. Mater Sci Technol 9(7):603–608
23. Mortezaie A, Shamanian M (2014) An assessment of microstructure, mechanical properties and corrosion resistance of dissimilar welds between Inconel 718 and 310S austenitic stainless steel. Int J Press Vessels Pip 116:37–46
24. Zhang Y, Fan M, Ding K, Zhao B, Zhang Y, He Y, Wang Y, Wu G, Wei T, Gao Y (2020) Formation and control of the residual δ-ferrite in 9% Cr-HAZ of Alloy 617/9% Cr dissimilar welded joint. Sci Technol Weld Joining 25(5):398–406
25. Mittal R, Sidhu BS (2015) Microstructures and mechanical properties of dissimilar T91/347H steel weldments. J Mater Process Technol 220:76–86
26. Sirohi S, Pandey C, Goyal A (2021) Role of the Ni-based filler (IN625) and heat-treatment on the mechanical performance of the GTA welded dissimilar joint of P91 and SS304H steel. J Manuf Process 65:174–189

Book Chapter

27. Taraphdar PK, Mahapatra MM, Pradhan AK, Singh PK, Sharma K, Kumar S (2021) Measurement of through-thickness residual stresses under restrained condition in pressure vessel steel weld. In: Saran VH, Misra RK (eds) Advances in systems engineering. lecture notes in mechanical engineering. Springer, Singapore pp 119–125

Journal Article

28. Das Banik S, Kumar S, Singh PK, Bhattacharya S, Mahapatra MM (2021) Distortion and residual stresses in thick plate weld joint of austenitic stainless steel: experiments and analysis. J Mater Process Technol 289: 116944

Journal Article by DOI (Before Issue Publication with Page Numbers)

29. Taraphdar PK, Kumar R, Pandey C, Mahapatra MM (2021) Significance of finite element models and solid-state phase transformation on the evaluation of weld induced residual stresses. Met Mater Int. https://doi.org/10.1007/s12540-020-00921-4

Journal Article

30. Taraphdar PK, Mahapatra MM, Pradhan, AK, Singh PK, Sharma K, Kumar S (2021) Effects of groove configuration and buttering layer on the through-thickness residual stress distribution in dissimilar welds. Int J Press Vessels Pip 192:104392
31. Dak G, Pandey C (2021) Experimental investigation on microstructure, mechanical properties, and residual stresses of dissimilar welded joint of martensitic P92 and AISI 304L austenitic stainless steel. Int J Press Vessels Pip 194:104536

A Methodology for Data-Driven Estimation of Forging Load

Kaustabh Chatterjee, Uday S. Dixit, Jian Zhang, and Pavel A. Petrov

Abstract Metal forming industry often requires to estimate forging load. Analytical and numerical techniques are not sufficient to provide an accurate estimation of the forging load. Interestingly, a large amount of shop floor forging data exists that are yet to be effectively utilised. Modelling using data-driven techniques can take care of the uncertainty associated with flow stress and friction condition. This article proposes a methodology that uses the existing information of axisymmetric forged products for the estimation of forging load by suggesting a proper value of complexity factor. Appropriate complexity factor is essential for empirically estimating the forging load in open as well as closed die forging. Estimation of forging load for open die forging is carried out for four different materials of cylindrical shape. In case of closed die forging, estimation of forging load is carried out for two different products. Forging load estimation is carried out for different sizes and for different friction conditions. The proposed methodology of using the existing data provides reasonable accuracy in the prediction of forging load.

Keywords Forging load · Complexity factor · Friction · Open die forging · Closed die forging · Axisymmetric product

K. Chatterjee (✉) · U. S. Dixit
Department of Mechanical Engineering, Indian Institute of Technology Guwahati, Guwahati 781039, India
e-mail: kaustabh@iitg.ac.in

U. S. Dixit
e-mail: uday@iitg.ac.in

J. Zhang
Shantou Institute of Light Industrial Equipment Research, Shantou University, Shantou-515063, China
e-mail: jianzhang@stu.edu.cn

P. A. Petrov
Department of Material Forming and Additive Technologies, Moscow Polytechnic University, str. B. Semenovskaya 38, 107023 Moscow, Russia

H. K. Dave et al. (eds.), *Recent Advances in Manufacturing Processes and Systems*, Lecture Notes in Mechanical Engineering,
https://doi.org/10.1007/978-981-16-7787-8_2

1 Introduction

Forging is one of the most popular manufacturing processes. It is a bulk metal forming process that is subjected to three-dimensional compressive stresses. Estimation and control of metal forging process are of utmost importance, particularly in this era of global competition. Researchers have been carrying out estimation of forging load, mostly using analytical, numerical and empirical methods. Such efforts are still continuing [1–3]. The deformation mechanics of forging is extremely complex. Additionally, the material flow is non-steady and non-uniform. However, with time, there has been sufficient progress in the field of analytical modelling that can accurately estimate the forging load. The main challenges in using analytical models are that they require the exact knowledge of the material behaviour during deformation and Coulomb's coefficient of friction. Assumptions such as homogenous deformation, temperature distribution due to different factors within and close to the deformation zone, and loading axes coinciding with the principal axes may be far away from reality. These drawbacks of analytical models were taken care by numerical models. With the advancement of processing power of computers, numerical models such as finite element method (FEM) provided quick estimation of forging load without the need to carry out expensive experiments [4]. However, FEM simulations are computationally expensive and can take up several hours for simulating the forging of three-dimensional products with complicated geometry. Empirical models require a lot of data for accurate estimation of forging load. To overcome these problems, researchers have started to develop intelligent databases for estimating forging load. The advancement in automation and information technology provided a golden opportunity for the manufacturing industries to store and access large amount of data. Effective utilization of such large amount of data directly form the shop floor can be used for reliable prediction of forging load.

Manufacturing industries are trying to incorporate cloud computing, big data, mobile Internet, cyber-physical system (CPS) and Internet of things (IOT) in their systems [5]. This has created interest among the researchers across the globe towards data-driven smart manufacturing [6]. Effective utilisation of manufacturing data for accurate performance prediction reduces the unnecessary downtime. Reduction of downtime improves the existing revenue of the organisation. Recently, Chatterjee et al. [7] proposed a framework for the acquisition of manufacturing data with efficient storage and performance prediction.

There are a few attempts in the past that proposes the usage of expert system for timely and effective utilisation of the accumulated data in forging. One of the initial works in expert system was carried out by Osakada and Yang [8]. They used backpropagation neural network aided expert system for determining the forming method, number of forming steps and prediction of die fracture with die defect. Katayama et al. [9] developed an expert system for the process design of a cold forging process. Expert system was also applied for determining the sequence of steps in manufacturing a part through axisymmetric cold forging [10]. Considering the uncertainty in forging process, fuzzy logic was applied. Fuzzy logic was used for

the estimation of the dimensional errors occurring during actual forging operation [11]. Gangopadhyay et al. [12] incorporated fuzzy logic in their expert system for the prediction of forging load and axial stress. Gronostajski et al. [13] used an expert system for determining the various wear mechanisms that degrade the forging tools during hot forging. Recently, deep learning techniques are also used in cold forging for condition monitoring of the machines [14]. Thus, researchers are trying hard to effectively utilise data-driven technologies in forging.

In estimating the forging load, there are two uncertain parameters: flow stress and friction condition. Flow stress significantly influences the material flow in forging operation. Flow stress is generally modelled in the form of mathematical equation, whose parameters are determined from compression tests. However, modelling of friction is itself a challenging task [15]. A thorough knowledge and a lot of skill is required for the estimation of forging load using the existing analytical and numerical models. Data-driven techniques can be effective in taking care of the various uncertainties associated with forging such as friction condition and flow stress. With time and usage, data-driven models get updated and provide more accurate results based on the feedback received from the shop floor.

In this paper, the idea is to build a robust procedure that can be used for the estimation of load in an axisymmetric forging. The methodology uses the existing information after applying the suitable correction factor depending on the situation. In order to demonstrate the methodology, simulations are carried out in place of shop floor data for axisymmetric forging of open and closed die products. In a sense, FEM simulations provide a virtual factory environment for testing the methodology.

2 Methodology

It is observed that a lot of forging data exist within an organisation and the same is not effectively utilised. The present work proposes to use such existing data for building a database such that it can be used for the estimation of forging load. For demonstrating the proposed methodology, forging is simulated using a commercial finite element package, ABAQUS. The feedback of the forging load obtained from simulations are assumed to represent the data obtained from the shop floor. The scheme adopted for estimating the forging load in open and closed die forging is shown in Fig. 1 and is discussed in details. The computational scheme could be repeated several times, while the accuracy of the computation would be enhanced.

Fig. 1 Scheme for estimating forging load

2.1 Forging Load in Open Die Forging

The slab method analysis in upsetting an axisymmetric disk using Coulomb's model gives the following die pressure p at any radial coordinate r as [16]:

$$p = \sigma_o \exp\left\{\frac{2\mu}{H}(R - r)\right\}, \tag{1}$$

where σ_o is the flow stress, μ is the coefficient of friction, H is the height, R is the final radius of the disk and r is the radial coordinate. Total forging load P is obtained by integrating the die pressure p over the whole contact area of the disk with the platen and is expressed as

$$P = \frac{\sigma_o \pi H}{\mu}\left[\frac{H}{2\mu}\left\{\exp\left(\frac{2\mu R}{H}\right) - 1\right\} - R\right]. \tag{2}$$

An empirical relation for the estimation of forging load was given long back [17] as

$$P = C_p \sigma_o A_p, \tag{3}$$

where C_p is the complexity factor and A_p is the plan area of the forging including flash. The aim of this article is to suggest a suitable value of C_p such that it can be used for any forging case. Equating Eqs. 2 and 3, the shape complexity can be computed as

$$C_p = \frac{H}{\mu R^2}\left[\frac{H}{2\mu}\left\{\exp\left(\frac{2\mu R}{H}\right) - 1\right\} - R\right]. \tag{4}$$

On substituting Eqs. 4 in 3, the forging load is estimated. The suggested value of the complexity factor is applicable for any sizes and for any friction condition.

2.2 Forging Load in Closed Die Forging

For closed die forging also, estimation of forging load is carried out using Eq. 3. However, it is difficult to ascertain an exact value of the C_p for an accurate load estimation. In general, the value of C_p is determined by intuition or experience. As already highlighted, the main aim of this article is to suggest a suitable value of C_p based on relevant product information. The idea is to effectively use the existing product information related to size and friction condition for predicting the forging load with reasonable accuracy.

2.2.1 Forging Load Estimation for Different Sizes of Workpieces

Assume that there are two models of similar shape but of different sizes. One model is having smaller radius (of projected circle) than the other. Assume that the existing information of the forging load is available for the smaller model under lubricated condition. It is required to estimate the forging load of a model having larger radius. However, height and friction condition are unchanged. Using Eq. 3, the forging load P for the large model is estimated as

$$P_{\text{large}} = \left(\frac{R_{\text{large}}}{R_{\text{small}}}\right)^2 \times P_{\text{small}}. \tag{5}$$

where R is the radius of the closed die product. In this case, the smaller model is considered as the base model, as prediction is carried out based on the information available of the smaller model. Similar methodology is adopted when information of larger model exists and estimation is required for smaller model by considering larger model as the base. On obtaining the actual load, the value of the complexity factor C_{p} is preserved. Such C_{p} is used for the estimation of forging load for a completely new product with different geometry. The value of C_{p} is again updated and preserved based on the feedback of the actual load.

2.2.2 Forging Load Estimation for Different Friction Condition

It is assumed that there are two models of similar shape and size. However, the information of lubricated condition exists. It is required to estimate the forging load under non-lubricated condition. In order to include the effect of friction in Eq. 4, a rough idea of the complexity factor C_{p} is required. The value of C_{p} for open die forging is approximately expressed by Eq. 4. Hence, C_{p} for closed die forging of non-lubricated case is obtained as

$$\begin{aligned}\left(C_{\text{p}}\right)_{\text{closed-nonlubriacted}} &= \frac{C_{\text{p}} \text{ from Eq. 4 for } \mu \text{ of non-lubricated case}}{C_{\text{p}} \text{ from Eq. 4 for } \mu \text{ of lubricated case}} \\ &\times \left(C_{\text{p}}\right)_{\text{closed-lubriacted}}.\end{aligned} \tag{6}$$

In this case, the lubricated model is considered as the base model, as prediction is carried out on the basis of the information of the lubricated model. Similar methodology is adopted to estimate the forging load for lubricated condition when data of non-lubricated condition is available. On obtaining the actual load, the value of the complexity factor C_{p} is preserved for the specified friction condition for further use. It is observed that estimating forging load considering the geometrically closest shape as the base model provide better accuracy in the prediction. A detailed insight is provided in the next section.